Petroleum Science 20 (2023) 1608–1619

Contents lists available at ScienceDirect

Petroleum Science

journal homepage: www.keaipublishing.com/en/journals/petroleum-science

Original Paper

Investigation of feasibility of alkali–cosolvent flooding in heavy oil reservoirs

Yi-Bo Li [a, *], He-Fei Jia [a], Wan-Fen Pu [a], Bing Wei [a, **], Shuo-Shi Wang [a, b], Na Yuan [b]

[a] State Key Laboratory of Oil and Gas Reservoir Geology and Exploitation, Southwest Petroleum University, Chengdu, 610500, Sichuan, China
[b] Mewbourne School of Petroleum and Geological Engineering, University of Oklahoma, Norman, OK, 73019, USA

ARTICLE INFO

Article history:
Received 31 August 2022
Received in revised form
1 December 2022
Accepted 1 December 2022
Available online 5 December 2022

Edited by Yan-Hua Sun

Keywords:
Heavy oil
Microemulsion
Cold production
Chemical flooding
Displacement efficiency

ABSTRACT

Cold production is a challenge in the case of heavy oil because of its high viscosity and poor fluidity in reservoir conditions. Alkali–cosolvent–polymer flooding is a type of microemulsion flooding with low costs and possible potential for heavy oil reservoirs. However, the addition of polymer may cause problems with injection in the case of highly viscous oil. Hence, in this study the feasibility of alkali–cosolvent (AC) flooding in heavy oil reservoirs was investigated via several groups of experiments. The interfacial tension between various AC formulations and heavy crude oil was measured to select appropriate formulations. Phase behavior tests were performed to determine the most appropriate formulation and conditions for the generation of a microemulsion. Sandpack flooding experiments were carried out to investigate the displacement efficiency of the selected AC formulation. The results showed that the interfacial tension between an AC formulation and heavy oil could be reduced to below 10^{-3} mN/m but differed greatly between different types of cosolvent. A butanol random polyether series displayed good performance in reducing the water–oil interfacial tension, which made it possible to form a Type III microemulsion in reservoir conditions. According to the results of the phase behavior tests, the optimal salinity for different formulations with four cosolvent concentrations (0.5 wt%, 1 wt%, 2 wt%, and 3 wt%) was 4000, 8000, 14000, and 20000 ppm, respectively. The results of rheological measurements showed that Type III microemulsion had a viscosity that was ten times that of water. The results of sandpack flooding experiments showed that, in comparison with waterflooding, the injection of a certain AC formulation slug could reduce the injection pressure. The pressure gradient during waterflooding and AC flooding was around 870 and 30–57 kPa/m, respectively. With the addition of an AC slug, the displacement efficiency was 30%–50% higher than in the case of waterflooding.

1. Introduction

Heavy oil resources are abundant throughout the world. According to statistics, the total reserves of crude oil worldwide are about 9–11 trillion barrels, of which heavy oil and bitumen resources comprise about two-thirds. Canada and Venezuela possess 40% of the world's heavy oil and bitumen resources (Dong et al., 2019; Li et al., 2021). In contrast to light oil, heavy oil has high viscosity and low fluidity as a result of its high contents of resin and asphaltene. Therefore, reducing viscosity and improving fluidity are the main methods used to develop heavy oil resources. Considering the temperature sensitivity of the characteristics of heavy oil, thermal recovery has always been the main method used for the recovery of heavy oil. The disadvantages of thermal oil recovery are high energy consumption and massive emissions of greenhouse gases. Therefore, cold production, which involves low energy consumption and causes little pollution, has gradually attracted attention. In recent years, the policy of reducing carbon dioxide emissions and CO_2 has a characteristics of miscibility with oil under certain conditions make gas flooding with CO_2 injection become the main method for oil development and enhance oil recovery. The success of CO_2 injection for improving shale oil recovery has been reported in many studies (Jin et al., 2017; Jia et al., 2019). An important reason is nanoporous structure of shale can increase the adsorption of CO_2 (Sander et al., 2020). Jia et al. also found that the

* Corresponding author.
** Corresponding author.
E-mail address: liyibo@swpu.edu.cn (Y.-B. Li).

https://doi.org/10.1016/j.petsci.2022.12.001

adsorption outweights molecular diffusion when considering the injection rate of CO_2 (Jia et al., 2022). Considering the large pore structure of conventional heavy oil reservoirs and the large viscosity difference between CO_2 and heavy oil, gas channel is easy to occur after CO_2 injection into heavy oil reservoir, which will result in an unsatisfactory sweep efficiency. This makes CO_2 flooding in heavy oil reservoirs questionable.

Recently, chemical flooding is the most popular conventional method used for cold production of heavy oil because of its good performance in reducing interfacial tension (IFT) and emulsifying and thus reducing the viscosity of heavy oil (Hirasaki et al., 2011; Liu et al., 2020). In China, oil production via enhanced oil recovery (EOR) accounted for 15%–18% of total oil production in recent years, and chemical flooding is currently the main method of EOR (Guo et al., 2018a, b; Li et al., 2021). According to statistics, oil production by chemical flooding accounted for 1.51% of total oil production worldwide, and in China this proportion has already reached 54.72% (Liu et al., 2020). The mechanism of viscosity reduction and EOR methods of heavy oil has been revealed through displacement experiments of different dimensions in laboratory (Wei et al., 2020; Guerrero et al., 2021). Alkali–surfactant–polymer (ASP) flooding has always been the main technique used for chemical flooding because of its unique advantages of improving the macro-sweep efficiency and micro-displacement efficiency. The addition of alkalis can also generate surfactants *in situ* with acidic components of crude oil to increase the micro-displacement efficiency (Flaaten et al., 2009; Fu et al., 2016; Nadeeka et al., 2018). Winsor defined four kinds of phase behavior (Magzymov et al., 2016). Type III microemulsion formed under suitable conditions has a high ability to solubilize crude oil and is generally considered to have the lowest IFT between any two phases among water, crude oil, and the microemulsion. The IFT between two phases can be calculated using the Huh equation (Huh, 1979).

The mechanism of ASP flooding has been studied by many researchers in the laboratory in recent years (Abdelfatah et al., 2020; Battistutta et al., 2015; Chen et al., 2018; Fu et al., 2016; Han et al., 2019; Liyanage et al., 2012). The purpose of ASP flooding is to generate a microemulsion *in situ*, which can reduce the water–oil IFT and the viscosity of heavy oil and has a certain ability to solubilize crude oil in reservoir conditions. The performance of ASP flooding in harsh reservoir conditions (high temperature, high salinity, and high brine hardness) has also been considered by changing the structure of the surfactant and the type of alkali used (Adkins et al., 2012; Lu et al., 2014a, b; Yang et al., 2010). Recently, Quintero et al. found that microemulsion can repair of near-wellbore fluid damage and dissolve asphaltene as a result of their characteristics of high oil solubilization rates and low IFT with crude oil (Quintero, 2020; Quintero et al., 2009, 2018). Because microemulsion can dissolve asphaltene, the success of microemulsion flooding in light oil reservoirs provided a new suggestion for microemulsion flooding in heavy oil reservoirs. Some researchers have carried out preliminary investigations of ASP flooding in heavy oil reservoirs (Aminzadeh et al., 2016; Kumar et al., 2012; Kumar Rahul and Mohanty, 2010; Pei et al., 2012; Sim et al., 2014; Zhang et al., 2012). These studies showed the strong potential of cold production in heavy oil reservoirs. More than 30 years have passed since the first field application of ASP flooding, and a fundamental understanding of its mechanism in EOR has already been achieved. The first field application of ASP flooding was reported in the United States in 1981, in which high-pH alkaline silicates were injected to enhance micellar polymer flooding, which was the earliest form of ASP flooding (Holm and Robertson, 1981). The first real test of ASP flooding in the field was in the West Kiehl Field, Wyoming, USA, in 1987 (Clark et al., 1993). The successful application of ASP flooding in field testing recovered more than 26% of the original oil in place (OOIP) within 2.5 years.

However, the major disadvantage of ASP flooding is the high cost of synthetic surfactants (Guo et al., 2018). Therefore, a novel cold production technique termed alkali–cosolvent–polymer (ACP) flooding, which uses no synthetic surfactants, has been developed. In comparison with ASP flooding, ACP flooding has lower costs because it uses a cheaper cosolvent instead of a surfactant but has a similar oil displacement mechanism. By the generation of natural surfactant with acidic components of crude oil, a Type III microemulsion can be formed with the cosolvent, natural surfactant, salt, and heavy oil. The polymer in the ACP slug is only used to increase the viscosity of the alkali–cosolvent (AC) formulation in the slug and does not participate in the reaction with heavy oil. Thus far, this technique has been validated by successful cases in several studies, which demonstrated the high displacement efficiency and low cost of ACP flooding (Aitkulov et al., 2016, 2017; Fortenberry et al., 2015; Sharma et al., 2018; Su et al., 2022).

As in the case of alkaline flooding, in order to generate a sufficient amount of natural surfactant the acid number of crude oil must be higher than 0.5 mg KOH/g oil (Graue and Johnson, 1974; Raimondi et al., 1977; Schumi et al., 2020). The cosolvent plays important roles in ACP flooding, such as promoting rapid equilibration, improving the phase behavior, broadening the optimal salinity range, maintaining rheological characteristics, and reducing the viscosity of the microemulsion (Chang et al., 2016; Pei et al., 2014; Sahni et al., 2010; Tagavifar et al., 2017a, b; Walker et al., 2012). The function of the polymer is to improve the injection profile of the injected fluid. However, according to previous research, the polymer is not involved in the reaction of crude oil with the chemical formulation. In a heavy oil reservoir, the addition of polymer may increase the difficulty of the injection of subsequent chemical slugs. On the other hand, it might affect the formation time of the microemulsion. For example, in the case of heavy oil reservoirs with a short well spacing, in particular, shallow heavy oil reservoirs in China with a well spacing of 100–150 m, a long reaction time is unfavorable. According to previous research, the viscosity of a microemulsion formed with light oil is higher than that of the oil itself, while the opposite is the case with heavy oil (Tagavifar et al., 2017a, b; Walker et al., 2012). In order to perform microemulsion flooding more effectively, it is usually combined with a high-viscosity solution to design a multi-slug flooding method (Najafi et al., 2017; Zhu et al., 2022). Adding polymer to the chemical slug is the commonest method of mobility control. In heavy oil reservoirs, decreases in reservoir permeability and increases in displacement pressure drop caused by retention of the polymer cannot be neglected. Thus, the chemical slug added polymer should have an appropriate viscosity. According to the results of most heavy oil polymer flooding and combined chemical flooding in laboratory and field tests in recent years, the viscosity of polymer slug is generally in the range of 10–30 mPa s (Delaplace et al., 2013; Gao, 2011a, b; Rousseau et al., 2018; Wassmuth et al., 2009; Wassmuth et al., 2007; Wu et al., 2011). For heavy oil, chemical flooding does not need to target a mobility ratio of unity to be efficient, but a tradeoff between mobility ratio and injectivity (Delamaide et al., 2014). Wang et al. studied the oil-induced viscoelastic behavior of an extended alkylpropoxy sulfate surfactant. The results showed that the injected fluid with oil-induced viscoelasticity provided not only ultralow oil–water IFT but also highly favorable rheological characteristics such as acting as polymer-free displacing agent which can possibly solve the problems of polymer injectivity and retention in heavy oil reservoirs (Chen et al., 2019, 2021). In addition, ACP flooding of viscous oil reservoirs was studied by numerical simulation using the UTCHEM simulator with 2D sandpacks, which also showed that ACP flooding

in heavy oil reservoirs is feasible (Aitkulov et al., 2017). All of the abovementioned studies proved the great potential and feasibility of AC flooding in heavy oil reservoirs.

The goal of this study was to develop an AC formulation without adding polymer for shallow heavy oil reservoirs with a short well spacing. We conducted tests of IFT and phase behavior between AC formulations and heavy oil. It was found that the IFT between the formulation and the heavy oil could be reduced to 10^{-3} mN/m and a Type III microemulsion was formed between the formulation and the heavy oil, which had an effect on fluidity control. Oil displacement tests were carried out in sandpacks, and the effect of the slug size was studied. Values of the main parameters, such as the pressure drop and cumulative oil recovery, were recorded and calculated. A high cumulative oil recovery and a reasonable pressure drop demonstrated the superior performance of the selected AC formulation.

Against the background of global warming and the high cost of thermal recovery, AC flooding, with its low cost and high efficiency, may represent a potential solution for cold production of heavy oil.

2. Experimental method

2.1. Materials

The heavy oil used in the experiments was kindly provided from the N6 block of the Xinjiang Oilfield, China. The relationship between the viscosity of the oil and the temperature is shown in Fig. 1. The viscosity of the oil was 1340 mPa s at 60 °C (current reservoir temperature). The total acid number was 2 mg KOH/g oil. Owing to the high acid number, an alkali could easily generate soap *in situ*. Several novel cosolvents that mainly consisted of derivatives of alcohols and ethers had high performance, which had been reported in many studies (Chang et al., 2016; Fortenberry et al., 2015; Nadeeka et al., 2018; Pei et al., 2014; Su et al., 2022). Therefore, in this study a butanol random polyether (BPE) series and isobutanol with ethylene oxide structure (IBA-*x*EO) series supplied by Haian Petrochemical Co., Ltd. Located in Nantong, China were used in primary screening of formulations. The molecular weights of the BPE were 1000 (BPE-1000) and 1600 (BEP-1600). The cosolvents were all hydrophilic with 10–30 ethoxy groups. The salinity of the water post-flush was around 4000 ppm, and the salts consisted primarily of NaCl. All brines were prepared by mixing laboratory-grade salts with deionized water. Because of the absence of divalent ions, sodium carbonate (Na_2CO_3) was chosen as the alkali. Sodium chloride and sodium carbonate with a purity of at least 99.5% were purchased from Chengdu Kelong Chemical, Chengdu, China. To prepare the chemical slug, the alkali and cosolvent were added to the brine.

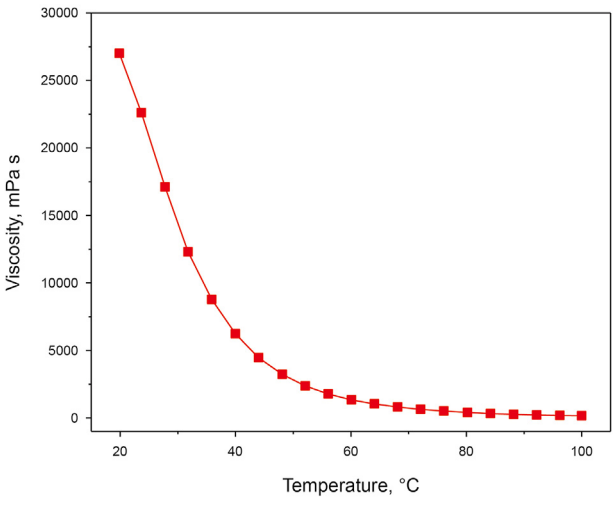

Fig. 1. Relationship between viscosity of heavy oil and temperature.

2.2. Interfacial tension measurements

This step involved preliminary screening of formulations by measuring the IFT between the AC solution and the heavy oil. The alkali–cosolvent–brine/oil IFT was determined using a spinning drop tensiometer (KRÜSS Scientific, Hamburg, Germany). Oil droplets and the AC solution were mixed and equilibrated at the experimental temperature (60 °C). Owing to the reaction between acidic components and the alkali, all the measurements lasted for at least 1 h. The instrument was equipped with image acquisition software by which IFT values could be calculated automatically according to parameters such as the volumes and diameters of the oil droplets. Different types of cosolvent were used. Formulations with ultralow IFT (of the order of 10^{-3} mN/m) would be considered as candidates for further investigation.

2.3. Phase behavior tests

The thermal stability of AC formulations was tested at 60 °C, and the aqueous stability was tested under conditions of different salinity. Salinity scans were performed to observe the miscibility between formulations and crude oil at reservoir temperature. Experiments were first performed to study the phase behavior of AC formulation–oil mixtures with changes in the alkali concentration. Aqueous solutions were prepared by mixing 0.5–3 wt% cosolvent with deionized water and alkali. The alkali concentration was varied systematically. An aliquot of 4 mL of each sample was pipetted into a thin graduated 10 mL borosilicate glass test tube with a diameter of 15 mm and a length of 120 mm, which avoided the capillary force that prevents crude oil and aqueous solutions from completely mixing. The level of the aqueous AC formulation without oil was recorded. Both the AC solution and the heavy oil were preheated in an oven at reservoir temperature. Before both the AC solution and the heavy oil had reached the predetermined temperature, 2 mL heavy oil was added to each test tube and the cap was tightened. The test tubes were then placed in an oven at reservoir temperature. To ensure that the heavy oil and AC solution were thoroughly mixed, all the samples were shaken once a day during the first few days. The phase behavior was then observed.

2.4. Rheological characteristics of microemulsion

In the absence of polymer, AC flooding incurs the risk of early water breakthrough as a result of the ultralow IFT. The viscosity of microemulsion was therefore measured to investigate the possibility of controlling the profile by an increase in viscosity. The rheological parameters of microemulsion were measured using a SmartPave dynamic shear rheometer (Anton Paar Co., Ltd, Graz, Austria). When the samples used for phase behavior testing were equilibrated, a syringe with a long needle was used to extract the microemulsion from the test tubes. A sample of about 2 mL was needed to complete a rheological test. A cone-and-plate geometry was used to measure viscosity at different shear rates at a fixed temperature. The viscosity was measured at shear rates ranging from 0.1 to 1000 s^{-1}. In order to exclude the influence of temperature on the phase behavior of microemulsion, all operations were carried out at 60 °C.

2.5. Sandpack flooding tests

Sandpack flooding tests were performed to test the performance of AC formulations in porous media. The pressure drop and recovery rate were considered as the main parameters. In order to prepare sandpacks for the flooding tests, a steel tube with a length of 0.45 m and a diameter of 0.02 m was packed with 60 mesh quartz sand. All fluid that entered a sandpack was pumped through an ISCO pump, which could control the injection flow rate, volume, and pressure. All preparation and displacement procedures were performed at 60 °C. The porosity was approximately 27.1%–35.5%. The permeability of sandpacks (1–2 D) was determined by injecting brine at 0.5 mL/min through the sandpacks and measuring the pressure drop between the two ends of the sandpacks using a Ps6000-3151 series intelligent pressure transmitter (Guangzhou Parsen Industrial Technology Co., Ltd, Guangzhou, China). Then the sandpacks were inverted, placed vertically, and saturated with crude oil at a rate of 0.1 mL/min. The properties of the sandpacks and injection slug parameters are shown in Table 1. Then the sandpacks were placed horizontally for displacement. AC flooding with different slug sizes followed by a 0.3–1 pore volume (PV) water post-flush was implemented to investigate the performance of the screened formulations. For comparison, a set of secondary waterflooding experiments was carried out. The AC formulation slug consisted of 3 wt% cosolvent and 2 wt% Na_2CO_3. The water post-flush slug contained 4000 ppm NaCl. The injection velocity in both AC flooding and the water post-flush was 0.025 mL/min, which corresponded to a field rate of 0.3 m/day. All sandpack flooding experiments were terminated at a water cut of 99%.

3. Results and discussion

3.1. Measurements of interfacial tension

To screen the appropriate AC solution for reducing IFT, the IFT between the oil and the alkali solution at concentrations of five types of cosolvent ranging from 0.5 to 3 wt% was measured and is plotted as a function of the Na_2CO_3 concentration in the range from 0 to 6 wt% in Fig. 2. At the same cosolvent concentration, the same trend was observed, namely, that the IFT value decreased first and subsequently increased with an increase in the alkali concentration. The minimum IFT value occurred at an alkali concentration of 1 wt% or 2 wt% Na_2CO_3. In the cases of the formulations containing any concentration of BPE-1000 and 2 wt% Na_2CO_3, the IFT could be reduced to the order of 10^{-3} mN/m, which was considered as ultralow. It can be observed that the IFT between an AC formulation containing 3 wt% BPE-1000 and heavy oil can be reduced greatly. The performance of the AC formulations containing the other four types of cosolvent was not as good as that of the AC formulation containing BPE-1000 as cosolvent, and the IFT was slightly higher than in the case of the formulation containing BPE-1000. The results of the IFT measurements indicated that there was strong synergy between the alkali and BPE-1000 in reducing the oil–water IFT. BPE-1000 was therefore selected as the cosolvent for the phase behavior experiments.

3.2. Results of phase behavior tests

Phase behavior tests (sodium carbonate scanning) were carried out to determine the optimal alkali concentration for the formulation and a suitable cosolvent concentration. Figs. 3–7 show the phase behavior of 0.5–3 wt% BPE-1000 with oil as the sodium carbonate concentration was varied at an oil/water volume ratio of 1:2. Acidic components of crude oil are partitioned between oil and water, and dissociation of acids forms soap, which can react with an alkali. Therefore, the amount of natural soap generated is mainly related to the amount of heavy oil. Due to the high viscosity of heavy oil, a small water/oil ratio will lead to a poor mixing results, which will hinder the sufficient chemical reaction between the AC formulation and crude oil, and cannot demonstration phase behavior results adequately. Therefore, the phase behavior experiments were carried out under an oil/water volume ratio of 1:2 (Ghosh and Johns, 2018; Khorsandi and Johns, 2018; Magzymov et al., 2021). The function of the cosolvent is to improve the overall hydrophilicity of soap because the natural soap generated by an alkali and acidic components of crude oil is usually hydrophobic. In addition, the transfer of soap between the oil and water phases is also associated with aqueous salinity. When the distribution of soap is balanced, a Type III microemulsion may be generated. At low salinity a Type I microemulsion formed by soap tends to transfer into the water phase, while at high salinity a Type II microemulsion formed by soap remains in the oil phase (Aitkulov et al., 2017). Four sets of phase behavior tests with different concentrations of cosolvent were conducted, and all the results for phase behavior are summarized in Fig. 3. With an increase in alkali concentration, all the sets of phase behavior tests showed a trend in the form of a transition of the microemulsion from Type I via Type III to Type II. It can be observed that the optimal salinity range became wider as the concentration of the cosolvent was increased. A wide optimal salinity range on a positive salinity gradient was considered favorable as the AC formulation slug was subsequently diluted by water during flooding. In this case, a Type III microemulsion could still exist. It can be seen from the results of interfacial tension data and phase state that the window of optimal salinity became wider with the increase of cosolvent concentration, however, there were cases that although the oil–water interfacial tension could be reduced to the order of 10^{-3} mN/m, which was considered as ultralow, no Type III microemulsion formed, for

Table 1
Properties of the sandpacks and injection slug parameters.

Test No.		#1	#2	#3	#4
Sandpack properties	Permeability, D	1.1	1.1	1.2	1.5
	Porosity, %	27.1	35.5	32.7	33.6
	Initial oil saturation, %	92	90	92.5	91.3
AC flooding	Slug size, PV	0	0.3	0.6	1.0
	Na_2CO_3 concentration, ppm	0	20000	20000	20000
	Cosolvent concentration, %	0	3	3	3
Water post-flush	Water post-flush size, PV	0.8	1.0	1.0	1.0
	Salinity as NaCl, ppm	4000	4000	4000	4000
	Flow rate, mL/min	0.025	0.025	0.025	0.025
Final oil recovery, %		22.9	54.7	64.5	75.0

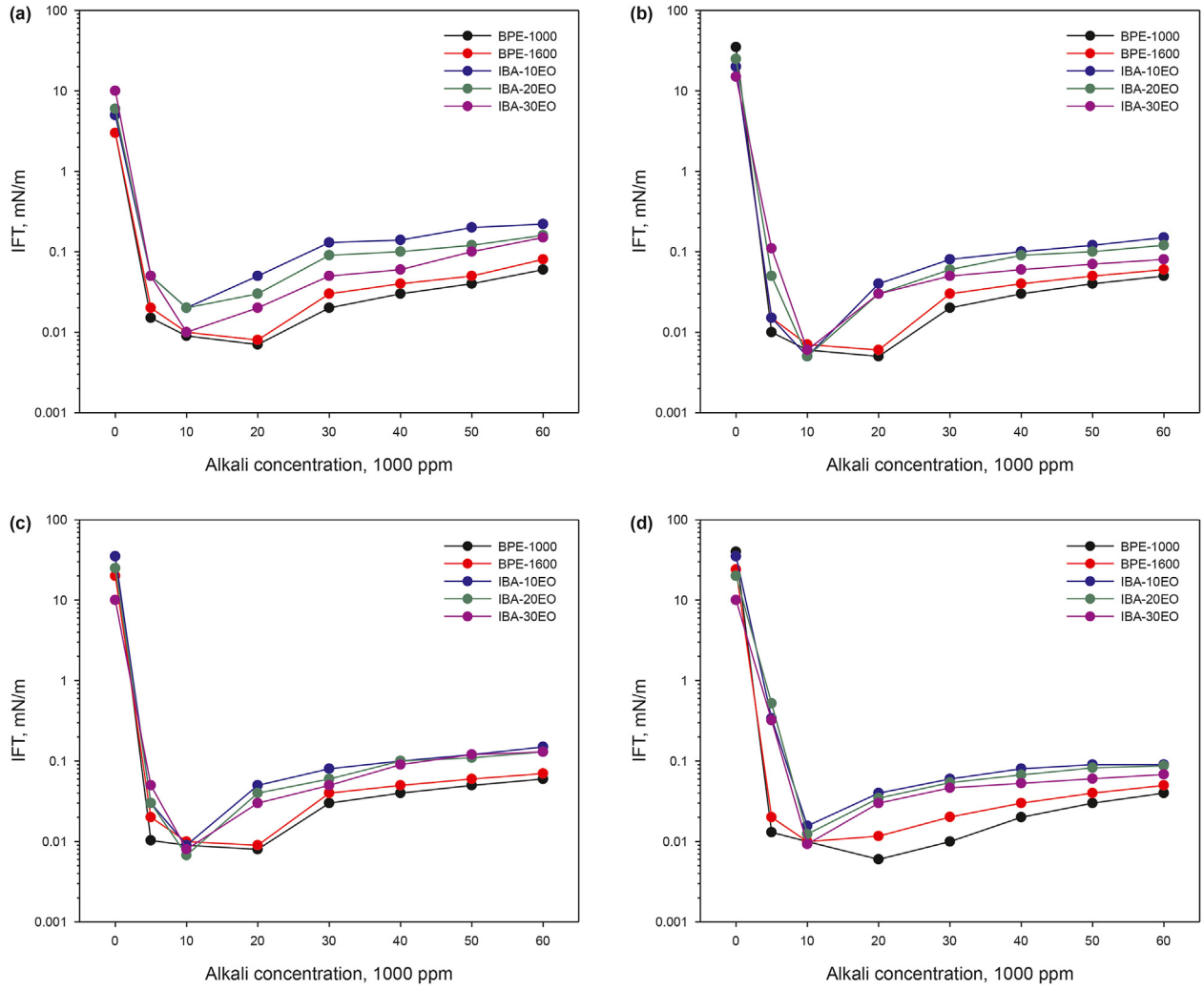

Fig. 2. Interfacial tension (IFT) between AC formulations with different concentrations of cosolvent ((**a**) 0.5 wt%, (**b**) 1 wt%, (**c**) 2 wt%, and (**d**) 3 wt%) and heavy oil.

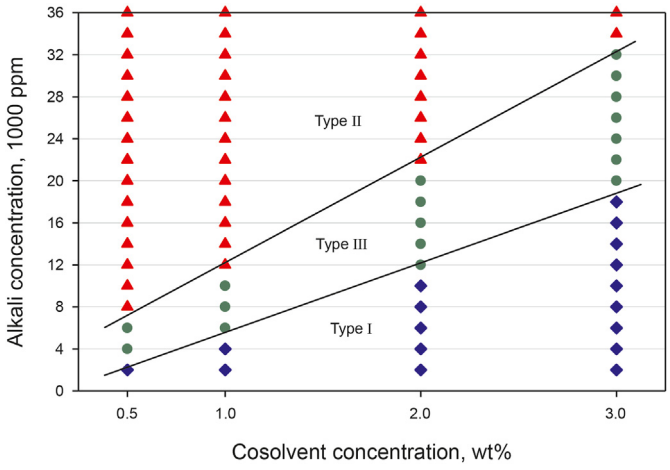

Fig. 3. Phase type and salinity range in phase behavior tests performed with different concentrations of cosolvent at 60 °C.

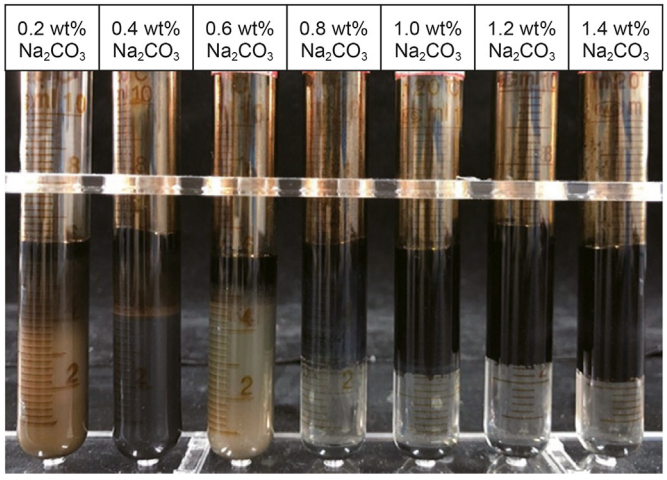

Fig. 4. Phase behavior of formulation containing 0.5 wt% BPE-1000 with oil at various alkali concentrations at 60 °C.

example, when the cosolvent concentration was 0.5 wt% at the salinity of 10000 ppm. Therefore, through the combination of interfacial tension and phase behavior results to understand the properties and behavior of the formulation mixed with the crude oil is an effective way to screen the formulation (Aitkulov and Mohanty, 2019; Liu et al., 2022; Magzymov et al., 2021; Nadeeka

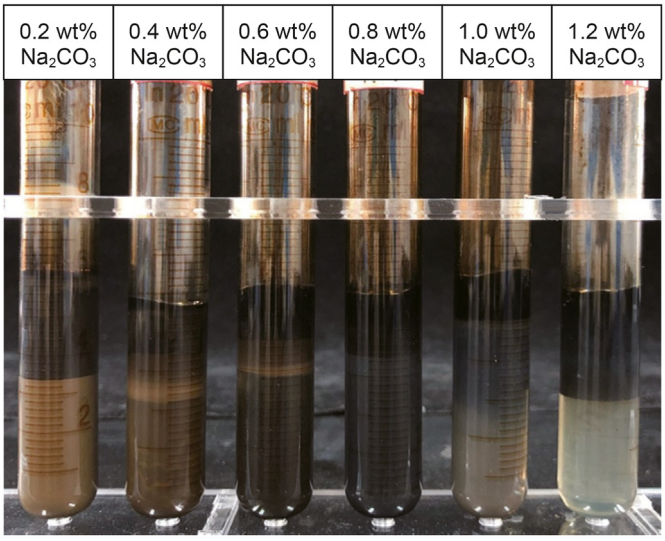

Fig. 5. Phase behavior of formulation containing 1 wt% BPE-1000 with oil at various alkali concentrations at 60 °C.

et al., 2018; Schumi et al., 2020; Zhao et al., 2020).

It took 7 days in the four sets of phase behavior tests for a Type III microemulsion to form. To further observe the stability of the phase behavior, after all the samples had been shaken once a day during the first few days, photos were taken after the samples had been left to stand for 30 days. Owing to the high content of asphaltene in heavy oil, the phase behavior results were different from those for kerosene and light oil, which usually formed a translucent middle phase (Chen et al., 2018; Evren et al., 2016; Hirasaki et al., 2011; Levitt et al., 2009). In the case of heavy oil, phase behavior with a gray-black or dark translucent underlayer tended to develop (Kumar et al., 2012; Kumar and Mohanty, 2010; Sim et al., 2014; Zhang et al., 2012). Fig. 4 shows the phase behavior with 0.5 wt% BPE-1000 as cosolvent with various alkali concentrations ranging from 0.2 wt% (on the left) to 1.4 wt% after 30 days. The optimal salinity for this formulation was 4000 ppm total dissolved solids (TDS), and the salinity range for Type III microemulsion was narrow. At low salinity (<4000 ppm), there were two phases: an excess oil phase and an aqueous phase containing soap, the cosolvent, and solubilized oil, which was considered to be a Type I microemulsion. As the salinity was increased, three phases

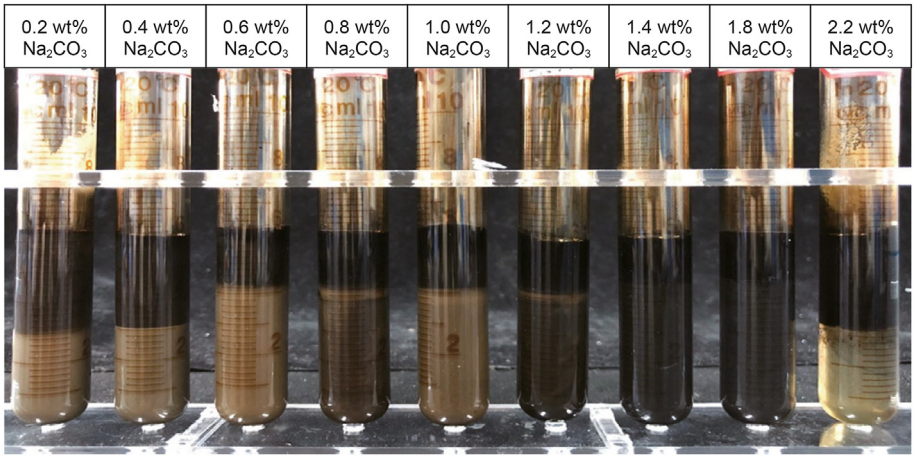

Fig. 6. Phase behavior of formulation containing 2 wt% BPE-1000 with oil at various alkali concentrations at 60 °C.

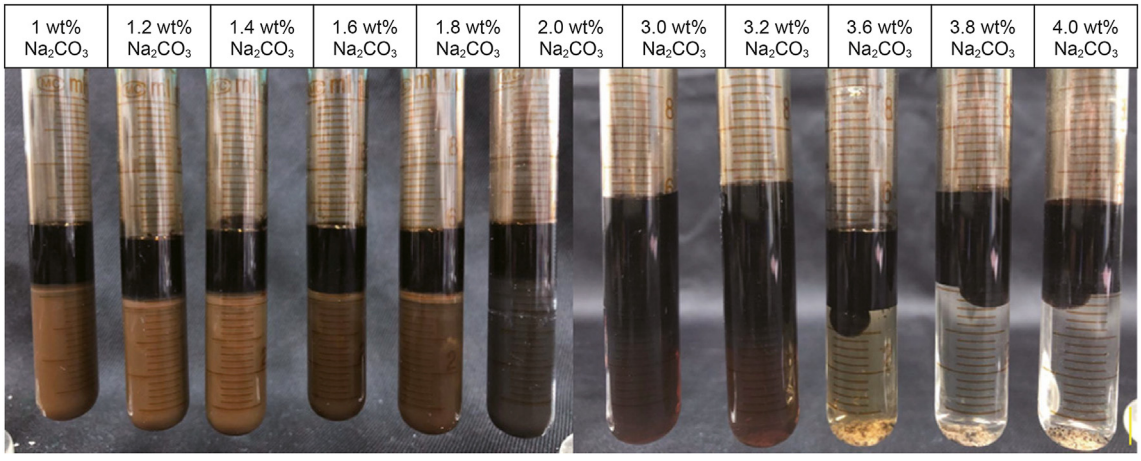

Fig. 7. Phase behavior of formulation containing 3 wt% BPE-1000 with oil at various alkali concentrations at 60 °C.

appeared: excess oil and water phases and a microemulsion. Part of the heavy oil was solubilized into a Type III microemulsion, and the underlayer was gray-black. The viscosity of Type III microemulsion was lower than that of heavy oil, and the fluidity was favorable. There will be opportunities for mobilization of heavy oil if a Type I or Type III microemulsion is formed under reservoir conditions. High salinity (>6000 ppm) led to a transition of the microemulsion from Type III to Type II. The phase behavior at the other three cosolvent concentrations exhibited the same trends, and the only difference was the optimal salinity value. Fig. 5 shows the phase behavior with 1 wt% BPE-1000 as cosolvent with various alkali concentrations ranging from 0.2 wt% (on the left) to 1.2 wt%. The optimal salinity for this formulation was 8000 ppm TDS, and the salinity range for Type III microemulsion was slightly wider than previously. A gray-black underlayer was observed in the salinity range of 0.6–0.8 wt%. Fig. 6 shows the phase behavior with 2 wt% BPE-1000 as cosolvent with various alkali concentrations ranging from 0.2 wt% (on the left) to 2.2 wt%. The optimal salinity for this formulation was 14000 ppm TDS, and the salinity range for Type III microemulsion was markedly wider than in the previous two experiments. A gray-black underlayer was observed in the salinity range of 1.2–1.8 wt%. Fig. 7 shows the phase behavior with 3 wt% BPE-1000 as cosolvent with various alkali concentrations ranging from 1 wt% (on the left) to 4 wt%. The optimal salinity for this formulation was 20000 ppm TDS, and the salinity range for Type III microemulsion was the widest in the four sets of phase behavior experiments. A gray-black or dark translucent underlayer was observed in the salinity range of 2–3.2 wt%. A wide salinity range for a Type III microemulsion is considered favorable and can improve the robustness of AC flooding during the displacement stage in situations where the salinity and cosolvent concentration change. Therefore, to ensure that the experimental data were more robust and clearer, the formulation containing 3 wt% cosolvent was further used for rheology measurements and displacement experiments. Relevant experiments with a lower concentration of cosolvent are under way. Although it took about 7 days to form Type III microemulsion during the phase behavior tests, due to the large specific surface inside the rock under reservoir conditions, the formulation will have more chances to contact with crude oil, which can result in speeding up the reaction rate between the formulation and crude oil and shortening the formation time of Type III microemulsion (Zhao et al., 2020, 2022).

3.3. Results of rheological characteristics of microemulsion

In order to understand whether a Type III microemulsion had the ability to control the profile in the absence of polymer, the viscosity of each phase of the microemulsion (the oil/water ratio was 1:2) formed by the AC formulation and heavy oil was tested using a rheometer. Fig. 8 shows the results for the viscosities of Type I, III, and II microemulsions from the phase behavior experiment performed with 3 wt% cosolvent and 20000 ppm alkali. Type I and Type III microemulsions had similar viscosities of around 10 mPa s at 60 °C, which were higher than the viscosity of water. As indicated in Section 1, the viscosity of the chemical slug is usually around 10–30 mPa s for medium-heavy oil reservoirs. Hence, a microemulsion slug with a viscosity of more than 10 mPa s may also have a certain mobility though the effect of mobility control may not be as good as adding polymer to chemical slug directly. Moreover, we did not rule out a viscous fingering phenomenon between the water phase and the microemulsion phase during the displacement process. However, the difference in viscosity between the microemulsion and water was much smaller than that between heavy oil and water. In addition, the sandpack was an approximate model of one-dimensional displacement, and hence a viscous

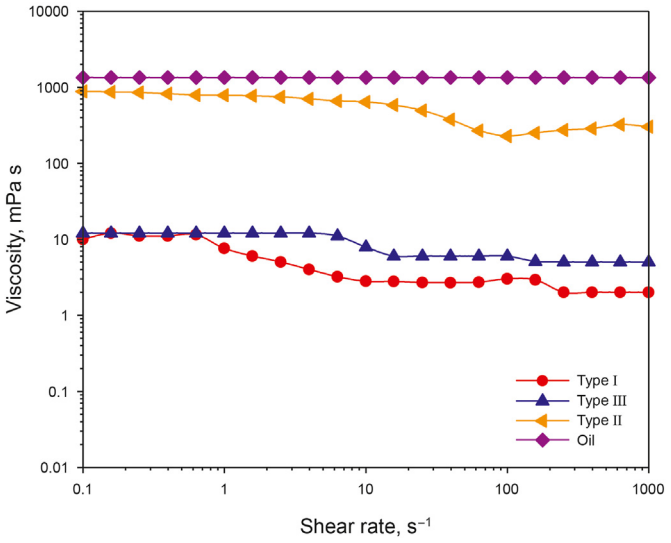

Fig. 8. Viscosities of Type I, Type II, and Type III microemulsions generated by formulation with 3 wt% BPE-1000 and heavy oil.

fingering phenomenon may still have occurred but was not so drastic. The viscosities of Type II microemulsion and heavy oil were approximately 900 and 1340 mPa s, respectively, at 60 °C. The results showed that Type III microemulsion generated by the AC solution and heavy oil had a certain ability to control fluidity without the addition of polymer. The cosolvent could improve the performance of the microemulsion and both Type I and Type III microemulsions were approximately Newtonian fluids at low shear rates.

3.4. Sandpack flooding tests study

AC flooding was tested in sandpacks and demonstrated promising results in the form of high oil recovery and a low pressure drop in comparison with waterflooding. The sandpacks were saturated with oil to an initial saturation of 90%–92.5%. In heavy oil reservoirs, the formation of dominant channels after waterflooding will have a negative effect on contact and reactions between the chemical formulation and crude oil. Therefore, the AC formulation was directly injected into the sandpack at a high oil saturation. According to the results of phase behavior tests, the optimal salinity (sodium carbonate concentration) of the formulation containing 3 wt% cosolvent was approximately 2 wt% sodium carbonate. Therefore, the salinity of the formulations was maintained at 2 wt% sodium carbonate in each of the following three sets of displacement experiments using AC formulations. The same slug combination (an AC formulation slug followed by a water post-flush slug) was used in all three sets of displacement experiments to compare the performance of AC flooding and waterflooding for the recovery of heavy oil.

3.4.1. Sandpack flooding test #1

In sandpack flooding test #1, waterflooding with a slug size of 0.8 PV was performed as a control procedure. The results for the cumulative oil recovery, oil cut, and pressure drop are shown in Fig. 9. The injection velocity was 0.025 mL/min, which corresponded to a field rate of 0.3 m/day. Owing to the high oil–water IFT and the huge difference in viscosity between the heavy oil and water, only 22.9% of the OOIP was recovered, and water breakthrough occurred at around 0.3 PV. The oil cut was reduced to less than 10% after 0.3 PV water was injected as a result of the water breakthrough. The oil cut and pressure drop began to decrease with

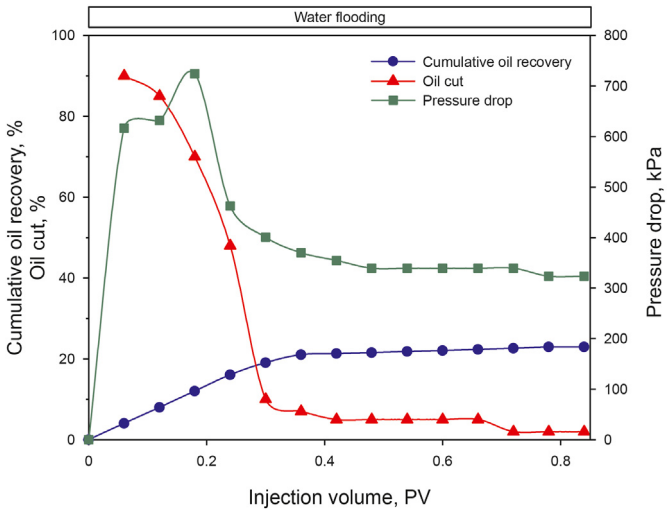

Fig. 9. Cumulative oil recovery, oil cut, and pressure drop of waterflooding with a slug size of 0.8 PV at 60 °C.

the water breakthrough (at about 0.3 PV). No more oil was recovered by waterflooding after water breakthrough, and thus the cumulative recovery did not change greatly. The average pressure gradient during the entire process was 870 kPa/m. In this case, if the well spacing is 100–150 m, the pressure drop between the injection well and the production well will reach about 87–130 MPa. Such a high injection pressure is impossible to achieve in the field. The pressure drop shown in Fig. 9 is the pressure drop between the two ends of the sandpack.

3.4.2. Sandpack flooding test #2

In sandpack flooding test #2, a 0.3 PV AC formulation slug followed by a 1 PV water post-flush slug was injected. The results for the cumulative oil recovery, oil cut, and pressure drop are shown in Fig. 10. The injection velocity in both AC flooding and the water post-flush was 0.025 mL/min, which corresponded to a field rate of 0.3 m/day. The salinity of the AC formulation slug and water post-flush slug was optimal and less than optimal, respectively. AC flooding recovered 33% of the OOIP. With the AC formulation, water breakthrough occurred at around 0.6 PV. The water post-flush still recovered 21.68% of the OOIP. This indicated that the AC formulation slug still maintained good performance although it had been diluted by subsequent waterflooding. The oil bank arrived at the outlet at about 0.05 PV after the AC formulation slug was injected. During the initial injection of the AC formulation slug, the oil cut in the effluent reached around 70%, and it decreased gradually at the end of the AC flooding. The oil cut in the waterflooding stage continued to decrease to close to 1%. At the beginning of the injection of the AC formulation slug, the pressure drop gradually increased to a peak value, and then it began to decrease and tended to become stable during the water post-flush stage. There was no considerable change in pressure drop during the water post-flush stage. The maximum pressure gradient was equal to 103 kPa/m. The minimum pressure gradient occurred in the waterflooding stage and was equal to 4.6 kPa/m. The pressure drop shown in Fig. 10 is the pressure drop between the two ends of the sandpack.

3.4.3. Sandpack flooding test #3

In sandpack flooding test #3, a 0.6 PV AC formulation slug followed by a 1 PV water post-flush slug was injected. The results for the cumulative oil recovery, oil cut, and pressure drop are shown in Fig. 11. The injection velocity in both AC flooding and the water post-flush was 0.025 mL/min, which corresponded to a field rate of 0.3 m/day. The salinity of the AC formulation slug and water post-flush slug was optimal and less than optimal, respectively. AC flooding recovered 61.4% of the OOIP. With the AC formulation, water breakthrough occurred at around 0.52 PV. The water post-flush recovered 3.05% of the OOIP. This indicated that the 0.6 PV AC formulation slug had recovered almost all the oil that could be mobilized, and it would also have been diluted by subsequent waterflooding. The oil bank arrived at the outlet at about 0.05 PV after the AC formulation slug was injected. During the initial injection of the AC formulation slug, the oil cut in the effluent reached around 80%, and it decreased gradually at the end of the AC flooding. The oil cut in the waterflooding stage continued to decrease to close to 1%. At the beginning of the injection of the AC formulation slug, the pressure drop gradually increased to a peak value, and then it began to decrease and tended to become stable during the water post-flush stage. There was no considerable change in pressure drop in the water post-flush stage. The maximum pressure gradient was equal to 71 kPa/m. The minimum

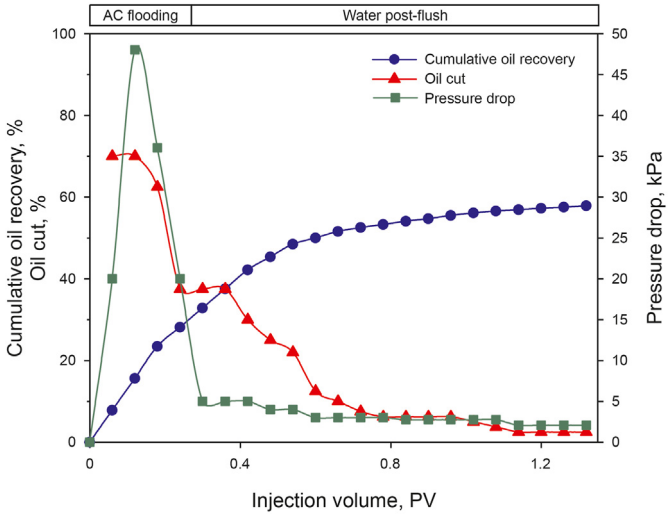

Fig. 10. Cumulative oil recovery, oil cut, and pressure drop in sandpack flooding test #2 with 0.3 PV AC formulation followed by a 1 PV water post-flush at 60 °C.

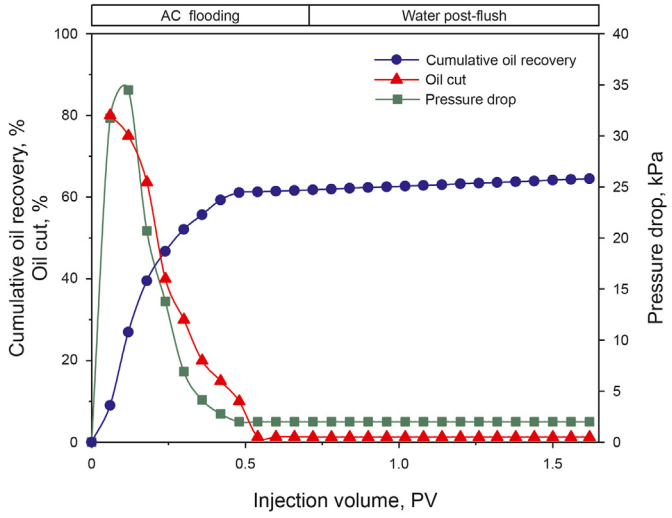

Fig. 11. Cumulative oil recovery, oil cut, and pressure drop in sandpack flooding test #3 with 0.6 PV AC formulation followed by a 1 PV water post-flush at 60 °C.

pressure gradient occurred in the water post-flush stage and was equal to 4.6 kPa/m. The pressure drop shown in Fig. 11 is the pressure drop between the two ends of the sandpack.

3.4.4. Sandpack flooding test #4

In sandpack flooding test #4, the effect of a 1 PV AC formulation slug followed by a 0.3 PV water post-flush slug was investigated. The results for the cumulative oil recovery, oil cut, and pressure drop are shown in Fig. 12. The injection velocity in both AC flooding and the water post-flush was 0.025 mL/min, which corresponded to a field rate of 0.3 m/day. The salinity of the AC formulation slug and water post-flush slug was optimal and less than optimal, respectively. AC flooding recovered 74% of the OOIP. With the AC formulation, water breakthrough occurred at around 0.5 PV. The water post-flush recovered 1% of the OOIP, and hence during the waterflooding stage only a further 1% of the OOIP could be recovered. At the end of the injection of the AC formulation slug, the oil cut decreased to close to 1%. This indicated that the large AC formulation slug recovered almost all the oil that could be mobilized. The oil cut in the subsequent water post-flush stage was low. A water post-flush slug of only 0.3 PV was injected because continued waterflooding had little effect on the cumulative recovery. The oil bank arrived at the outlet at about 0.05 PV after the AC formulation slug was injected. During the initial injection of the AC formulation slug, the oil cut in the effluent reached around 75%, and it decreased gradually at the end of the AC flooding. The oil cut in the waterflooding stage continued to decrease to close to 1%. At the beginning of the injection of the AC formulation slug, the pressure drop gradually increased to a peak value, and then it began to decrease and tended to become stable during the water post-flush stage. There was no considerable change in pressure drop in the water post-flush stage. The maximum pressure gradient was equal to 175 kPa/m. The minimum pressure gradient occurred in the waterflooding stage and was equal to 4.6 kPa/m. The pressure drop shown in Fig. 12 is the pressure drop between the two ends of the sandpack. The results of sandpack flooding test #4 confirmed that the application of a large chemical slug could result in higher oil recovery. The influence of the water post-flush after a sufficient AC formulation slug had been injected on cumulative recovery was negligible because the oil cut was close to 1% in the later period of injection of the AC formulation slug and the entire water post-flush stage.

3.4.5. Discussion of displacement results

Displacement pressure drop and cumulative oil recovery are critical parameters for cold production of heavy oil. A comparison of the results for the cumulative oil recovery is shown in Fig. 13. The cumulative oil recovery after waterflooding in sandpack flooding test #1 was only 22.9%. In the other three sets of sandpack flooding tests with AC formulations, the cumulative oil recovery was positively correlated with the size of the AC formulation slug that was injected. Most of the oil was recovered during AC flooding, in which the contribution of the AC formulation slug to the cumulative oil recovery became increasingly smaller. The contribution of the water post-flush to the cumulative oil recovery decreased with an increase in the size of the AC formulation slug because AC flooding had recovered almost all of the oil that could be mobilized by a chemical formulation.

A comparison of the results for the pressure gradient is shown in Fig. 14. Owing to the high oil–water IFT and the huge difference in viscosity between the heavy oil and water, a huge pressure drop occurred during waterflooding. The maximum and average pressure gradients over the entire process were around 1.6 and 870 kPa/m, respectively. As mentioned for sandpack flooding test #1, the pressure drop between the injection well and the production well will reach around 87–130 MPa with a well spacing of 100–150 m. Such a high injection pressure is impossible to achieve in the field.

It can be observed that the pressure gradient gradually stabilized after 0.3 PV during waterflooding in sandpack flooding test #1. The average pressure gradient in the stable stage was still as high as around 0.75 MPa/m. However, the maximum pressure gradient ranged from around 71 to 175 kPa/m, whereas the average pressure gradient ranged from 30 to 57 kPa/m during AC formulation slug injected, which was only 1/29 to 1/15 of the value during waterflooding. In this case, the pressure drop between the injection well and the production well will reach about 3–5.7 MPa with a well spacing of 100 m and 4.5–8.55 MPa with a well spacing of 150 m, which is favorable. The average pressure gradient successively decreased with an increase in the size of the AC formulation slug, for which the reason was that the injection of a large amount of AC formulation slug lengthened the period of low-pressure displacement. The low average pressure gradient and acceptable maximum pressure gradient over the entire process of AC flooding demonstrated favorable ability for reducing the injection pressure

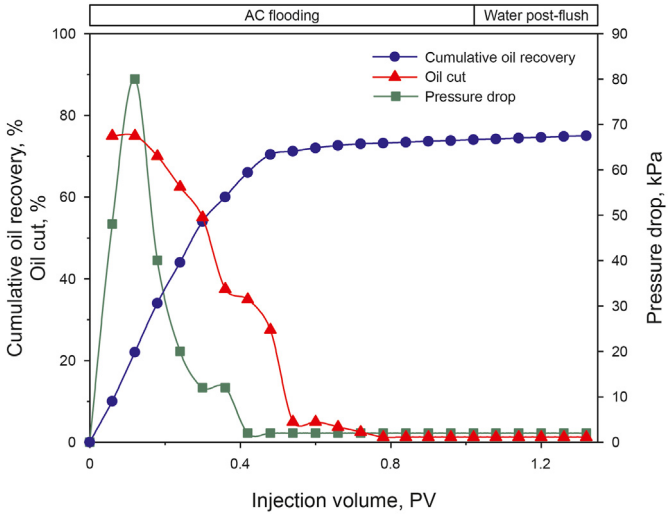

Fig. 12. Cumulative oil recovery, oil cut, and pressure drop in sandpack flooding test #4 with 1 PV AC formulation followed by a 0.3 PV water post-flush at 60 °C.

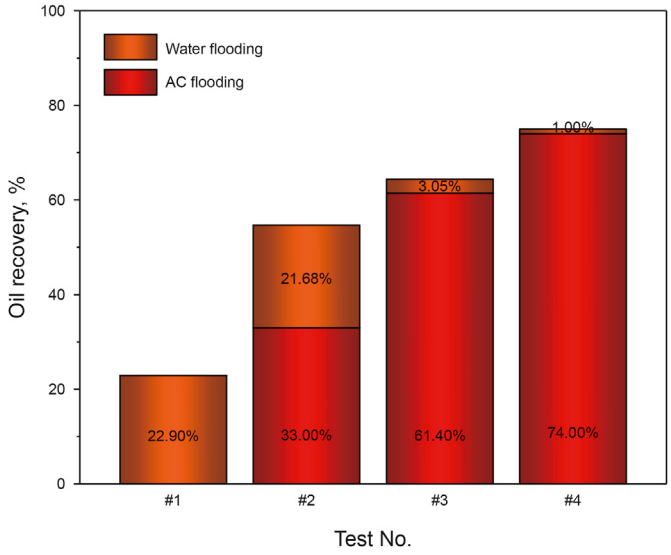

Fig. 13. Oil recovery values after AC flooding and the entire process in the four sets of sandpack flooding tests.

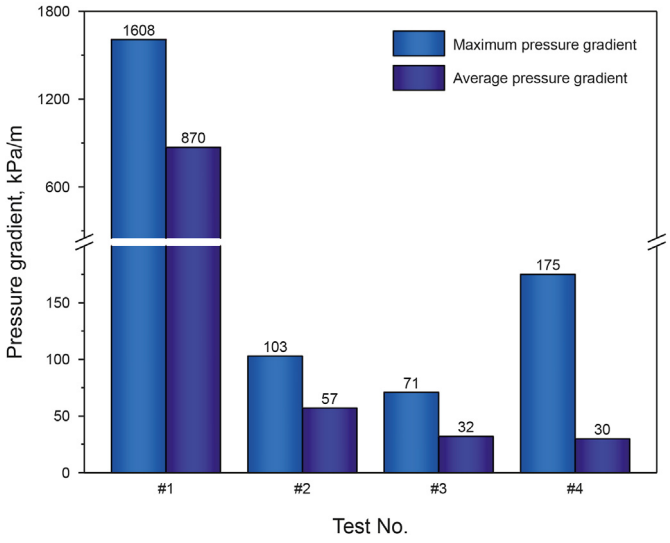

Fig. 14. Maximum pressure gradient and average pressure gradient during waterflooding and three sets of AC flooding.

in cold production of heavy oil.

A comparison of the results for the water breakthrough time is shown in Fig. 15. In sandpack flooding test #1, water breakthrough occurred at around 0.3 PV after water was injected. The breakthrough time in the three sets of AC flooding tests was markedly later than in the case of waterflooding. As indicated in Section 3.3, the viscosity of the microemulsion was higher than that of water, which provided a certain ability to control the profile. The reaction between the AC formulation and the heavy oil also took some time. In addition, wettability alteration due to the generation of natural soap may also increase the sweep efficiency of water. Although pore walls may be altered to become partially oil-wetted as a result of the formation of a water-in-oil (W/O) emulsion, and the viscosity of the W/O emulsion was much higher than that of the water phase and even higher than that of the oil phase, which can cause an increase in pressure drop, the smooth pressure drop curve for the water post-flush stage indicated that no W/O emulsion was formed,

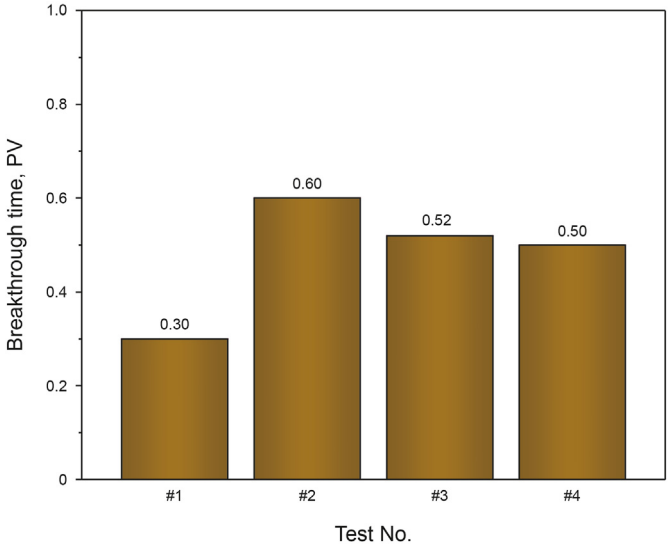

Fig. 15. Water breakthrough time after fluid injection during waterflooding and three sets of AC flooding.

which implied that the pore walls were altered to become water-wetted (Arhuoma et al., 2009; Dong et al., 2012). All of these factors resulted in a delay in water breakthrough in comparison with waterflooding.

3.4.6. Mechanism of AC flooding

An ultralow IFT, the formation of a Type III microemulsion, and a certain profile-controlling effect in the absence of polymer could be achieved between the AC formulation and the heavy oil according to the previous IFT tests, phase behavior tests, and rheology tests. The mechanism of ACP is that the chemical solution first generates an miscible zone between original oil and follow-up formulation slug which has an ability of mobility ratio improvement to mobilize oil and then dissolve and emulsify residual oil under ultralow interfacial tension (IFT) conditions (Su et al., 2022). From these properties and the results of the sandpack flooding tests, the mechanism of AC flooding in heavy oil could be described as follows: an AC formulation with ultralow IFT can be miscible with crude oil and the miscible zone will displace residual oil under ultralow interfacial tension (IFT) conditions, a type III microemulsion with a certain viscosity can not only solubilize crude oil but also has a certain ability to control the profile as indicated in Section 1 to mobilize oil and then the emulsion of the miscible zone trailing edge and residual oil are peeled off from pore wall due to wettability alteration.

3.5. Potential advantages of AC flooding

3.5.1. Advantages of AC flooding

In the process of heavy oil thermal production, heat loss and formation thermal conductivity must be considered. Some reservoir conditions limit the use of thermal production including thin-bedded reservoirs, bottom-water reservoirs, gas cap reservoirs and low rock thermal conductivity. There are significant heat losses in these reservoirs by thermal recovery. However, as one of the cold production methods, AC flooding is a low energy cost method because it does not require additional heat input and applicable to a wider range of reservoir conditions (Karmaker and Maini, 2003; Lin et al., 2014). In addition, heavy oil cold production eliminates the large amount of greenhouse gas emissions accompanying thermal production process (Lin et al., 2014; Luhning et al., 2003).

3.5.2. Economic efficiency

The AC technology uses cosolvent to replace synthetic surfactant if ASP technology is particularly promising for heavy oil, which can form amounts of soap. And surfactant is the most expensive chemical in these processes. Thus, selecting an cosolvent that can achieve the same or similar performance as synthetic surfactant and has lower cost is crucial, which was confirmed by many researchers (Fortenberry et al., 2015; Sharma et al., 2018). In addition, Schumi et al. also demonstrated the highest incremental recovery of ACP injection compared to alkali flooding, polymer flooding, and alkali/polymer flooding (Schumi et al., 2020). Chemical formulation selection based on these criteria provides a potential solution for low cost and high efficiency cold production of heavy oil.

4. Conclusions

An AC formulation prepared without the use of a synthetic surfactant exhibited excellent performance in a series of experiments with heavy oil at 60 °C. The main conclusions are as follows:

(1) Ultralow IFT can be achieved between an AC formulation and heavy oil without the use of synthetic surfactants.

(2) A Type III microemulsion can be formed between an AC formulation and heavy oil. Owing to the presence of asphaltene in heavy oil, the Type III microemulsion for heavy oil was different from that for light oil, and a gray-black or dark translucent underlayer tended to develop.
(3) The viscosity of the Type III microemulsion was about 10 mPa s, which had an effect on mobility control to a certain extent.
(4) The pressure gradients during AC flooding were reasonable, and the water post-flush made a negligible contribution to the cumulative oil recovery when a sufficient amount of the AC formulation had been injected.
(5) Three sets of AC flooding tests showed excellent performance for the recovery of heavy oil, as indicated by a high cumulative oil recovery, reasonable pressure gradients, and the potential for low costs in the absence of a synthetic surfactant. The advent of such a novel effective method significantly broadens the potential range of application of cold production for heavy oil reservoirs.

Declaration of competing interest

The authors declare that they have no known competing financial interests or personal relationships that could have appeared to influence the work reported in this paper.

Acknowledgement

The authors wish to recognize financial support from the National Natural Science Foundation of China (52174034) and the Sichuan Science and Technology Program (2021YFH0081).

References

Abdelfatah, E., Wahid-Pedro, F., Melnic, A., Vandenberg, C., Luscombe, A., Berton, P., Bryant, S.L., 2020. Microemulsion formulations with tunable displacement mechanisms for heavy oil reservoirs. SPE J. 25 (5), 2663–2677. https://doi.org/10.2118/196097-PA.
Adkins, S., Arachchilage, G.P., Solairaj, S., Lu, J., Weerasooriya, U., Pope, G.A., 2012. Development of thermally and chemically stable large-hydrophobe alkoxy carboxylate surfactants. In: SPE Improved Oil Recovery Symposium. https://doi.org/10.2118/154256-MS.
Aitkulov, A., Mohanty, K.K., 2019. Investigation of alkaline-surfactant-polymer flooding in a quarter five-spot sandpack for viscous oil recovery. J. Petrol. Sci. Eng. 175, 706–718. https://doi.org/10.1016/j.petrol.2019.01.018.
Aitkulov, A., Lu, J., Pope, G.A., Mohanty, K.K., 2016. Optimum time of ACP injection for heavy oil recovery. In: SPE Canada Heavy Oil Technical Conference. https://doi.org/10.2118/180757-MS.
Aitkulov, A., Luo, H.S., Lu, j, Mohanty, K.K., 2017. Alkali–Cosolvent–Polymer flooding for viscous oil recovery: 2D Evaluation. Energy Fuels 31 (7), 7015–7025. https://doi.org/10.1021/acs.energyfuels.7b00790.
Aminzadeh, B., Hoang, V., Inouye, A., Izgec, O., Walker, D., Chung, D., Nizamidin, N., Tang, T., Lolley, C., Dwarakanath, V., 2016. Improving recovery of a viscous oil using optimized emulsion viscosity. In: SPE Improved Oil Recovery Conference. https://doi.org/10.2118/179698-MS.
Arhuoma, M., Dong, M.Z., Yang, D.Y., Idem, R., 2009. Determination of water-in-oil emulsion viscosity in porous media. Ind. Eng. Chem. Res. 48 (15), 7092–7102. https://doi.org/10.1021/ie801818n.
Battistutta, E., Van Kuijk, S.R., Groen, K.V., Zitha, P.L., 2015. Alkaline-surfactant-polymer (ASP) flooding of crude oil at under-optimum salinity conditions. In: SPE Asia Pacific Enhanced Oil Recovery Conference. https://doi.org/10.2118/174666-MS.
Chang, L.Y., Lansakara-P, D.S., Jang, S.H., Weerasooriya, U.P., Pope, G.A., 2016. Co-solvent partitioning and retention. In: SPE Improved Oil Recovery Conference. https://doi.org/10.2118/179676-MS.
Chen, Z., Han, X., Kurnia, I., Yu, J.J., Zhang, G.Y., Li, L., 2018. Adoption of phase behavior tests and negative salinity gradient concept to optimize Daqing oilfield alkaline-surfactant-polymer flooding. Fuel 232, 71–80. https://doi.org/10.1016/j.fuel.2018.05.130.
Chen, C., Wang, S., Grady, B.P., Harwell, J.H., Shiau, B.J., 2019. Oil-induced viscoelasticity in micellar solutions of alkoxy sulfate. Langmuir 35 (37), 12168–12179. https://doi.org/10.1021/acs.langmuir.9b01969.
Chen, C.L., Wang, S.S., Harwell, J.H., Shiau, B.J., 2021. Polymer-free viscoelastic fluid for improved oil recovery. Fuel 292, 120331. https://doi.org/10.1016/j.fuel.2021.120331.
Clark, S.R., Pitts, M.J., Smith, S.M., 1993. Design and application of an alkaline-surfactant-polymer recovery system for the West Kiehl field. SPE Adv. Technol. 1 (1), 172–179. https://doi.org/10.2118/17538-PA.
Delamaide, E., Zaitoun, A., Renard, G., Tabary, R., 2014. Pelican Lake Field: first successful application of polymer flooding in a heavy-oil reservoir. SPE Reservoir Eval. Eng. 17 (3), 340–354. https://doi.org/10.2118/165234-PA.
Delaplace, P., Delamaide, E., Roggero, F., Renard, G., 2013. History matching of a successful polymer flood pilot in the Pelican Lake heavy oil field. In: SPE Annual Technical Conference and Exhibition. https://doi.org/10.2118/166256-MS.
Dong, M.Z., Liu, Q., Li, A.F., 2012. Displacement mechanisms of enhanced heavy oil recovery by alkaline flooding in a micromodel. Particuology 10 (3), 298–305. https://doi.org/10.1016/j.partic.2011.09.008.
Dong, X.H., Liu, H.Q., Chen, Z.X., Wu, K.L., Lu, N., Zhang, Q.C., 2019. Enhanced oil recovery techniques for heavy oil and oilsands reservoirs after steam injection. Appl. Energy 239, 1190–1211. https://doi.org/10.1016/j.apenergy.2019.01.244.
Evren, U., Marc, B., Ryan, T.A., 2016. Pore scale dynamics of microemulsion formation. Langmuir 32 (28). https://doi.org/10.1021/acs.langmuir.6b00821.
Flaaten, A.K., Nguyen, Q.P., Pope, G.A., Zhang, J.Y., 2009. A systematic laboratory approach to low-cost, high-performance chemical flooding. SPE Reservoir Eval. Eng. 12 (5), 713–723. https://doi.org/10.2118/113469-PA.
Fortenberry, R., Kim, D.H., Nizamidin, N., Adkins, S., Arachchilage, G.W.P., Koh, H., Weerasooriya, U., Pope, G.A., 2015. Use of cosolvents to improve alkaline/polymer flooding. SPE J. 20 (2), 255–266. https://doi.org/10.2118/166478-PA.
Fu, L.P., Zhang, G.C., Ge, J.J., Liao, K.L., Pei, H.H., Jiang, P., Li, X.Q., 2016. Study on organic alkali-surfactant-polymer flooding for enhanced ordinary heavy oil recovery. Colloid. Surface. 508, 230–239. https://doi.org/10.1016/j.colsurfa.2016.08.042.
Gao, C.H., 2011a. Advances of polymer flood in heavy oil recovery. In: SPE Heavy Oil Conference and Exhibition. https://doi.org/10.2118/150384-MS.
Gao, C.H., 2011b. Scientific research and field applications of polymer flooding in heavy oil recovery. J. Pet. Explor. Prod. Technol. 1 (2), 65–70. https://doi.org/10.1007/s13202-011-0014-6.
Ghosh, S., Johns, R.T., 2018. A modified HLD-NAC equation of state to predict alkali/surfactant/oil/brine phase behavior. SPE J. 23 (2), 550–566. https://doi.org/10.2118/175132-PA.
Graue, D.J., Johnson Jr., C.E., 1974. Field trial of caustic flooding process. J. Petrol. Technol. 26 (12), 1353–1358. https://doi.org/10.2118/4740-PA.
Guerrero, F., Bryan, J., Kantzas, A., 2021. Visualization of chemical heavy oil EOR displacement mechanisms in a 2D system. Energies 14 (4), 950. https://doi.org/10.3390/en14040950.
Guo, H., Dong, J.Y., Wang, Z.B., Liu, H.F., Ma, R.C., Kong, D.B., Wang, F.Y., Xin, X.K., Li, Y.Q., She, H.C., 2018a. 2018 EOR survey in China-Part 1. In: SPE Improved Oil Recovery Conference. https://doi.org/10.2118/190286-MS.
Guo, H., Li, Y.Q., Kong, D.B., Ma, R.C., Li, B.H., Wang, F.Y., 2018b. Lessons learned from alkali/surfactant/polymer flooding field tests in China. SPE Reservoir Eval. Eng. 22 (1), 78–99. https://doi.org/10.2118/186036-PA.
Han, X., Kurnia, I., Chen, Z., Yu, J.J., Zhang, G.Y., 2019. Effect of oil reactivity on salinity profile design during alkaline-surfactant-polymer flooding. Fuel 254. ARTN11573810.1016/j.fuel.2019.115738.
Hirasaki, G.J., Miller, C.A., Puerto, M., 2011. Recent advances in surfactant EOR. SPE J. 16 (4), 889–907. https://doi.org/10.2118/115386-PA.
Holm, L.W., Robertson, S.D., 1981. Improved micellar-polymer flooding with high-pH chemicals. J. Petrol. Technol. 33 (1), 161–172. https://doi.org/10.2118/7583-PA.
Huh, C., 1979. Interfacial tensions and solubilizing ability of a microemulsion phase that coexists with oil and brine. J. Colloid Interface Sci. 71 (2), 408–426. https://doi.org/10.1016/0021-9797(79)90249-2.
Jia, B., Tsau, J.S., Barati, R., 2019. A review of the current progress of CO_2 injection EOR and carbon storage in shale oil reservoirs. Fuel 236, 404–427. https://doi.org/10.1016/j.fuel.2018.08.103.
Jia, B., Chen, Z., Xian, C., 2022. Investigations of CO_2 storage capacity and flow behavior in shale formation. J. Petrol. Sci. Eng. 208, 109659. https://doi.org/10.1016/j.petrol.2021.109659.
Jin, L., Hawthorne, S., Sorensen, J., et al., 2017. Advancing CO_2 enhanced oil recovery and storage in unconventional oil play—experimental studies on Bakken shales. Appl. Energy 208, 171–183. https://doi.org/10.1016/j.apenergy.2017.10.054.
Karmaker, K., Maini, B.B., 2003. Applicability of vapor extraction process to problematic viscous oil reservoirs. In: SPE Annual Technical Conference and Exhibition. https://doi.org/10.2118/84034-MS.
Khorsandi, S., Johns, R.T., 2018. Extension of HLD-NAC flash calculation algorithm to multicomponent mixtures of microemulsion and excess phases. In: SPE Improved Oil Recovery Conference. https://doi.org/10.2118/190207-MS.
Kumar, R., Mohanty, K.K., 2010. ASP flooding of viscous oils. In: SPE Annual Technical Conference and Exhibition. https://doi.org/10.2118/135265-MS.
Kumar, R., Dao, E., Mohanty, K.K., 2012. Heavy-oil recovery by in-situ emulsion formation. SPE J. 17 (2), 326–334. https://doi.org/10.2118/129914-PA.
Levitt, D.B., Jackson, A.C., Heinson, C., Britton, L.N., Malik, T., Dwarakanath, V., Pope, G.A., 2009. Identification and evaluation of high-performance EOR surfactants. SPE Reservoir Eval. Eng. 12 (2), 243–253. https://doi.org/10.2118/100089-PA.
Li, Y.B., Wang, Z.Q., Hu, Z.M., Xu, B.Q., Li, Y.L., Pu, W.F., Zhao, J.Z., 2021. A review of in situ upgrading technology for heavy crude oil. Petroleum 7 (2), 117–122. https://doi.org/10.1016/j.petlm.2020.09.004.
Lin, L.X., Ma, H.Z., Zeng, F.H., Gu, Y.G., 2014. A critical review of the solvent-based

heavy oil recovery methods. In: SPE Heavy Oil Conference-Canada. https://doi.org/10.2118/170098-MS.
Liu, Z.X., Liang, Y., Wang, Q., Guo, Y.J., Gao, M., Wang, Z.B., Liu, W.L., 2020. Status and progress of worldwide EOR field applications. J. Petrol. Sci. Eng. 193. https://doi.org/10.1016/j.petrol.2020.107449.
Liu, J.B., Zhong, L.G., Hao, T.C., Liu, Y.G., Zhang, S.J., 2022. Pore-scale dynamic behavior and displacement mechanisms of surfactant flooding for heavy oil recovery. J. Mol. Liq. 349, 118207. https://doi.org/10.1016/j.molliq.2021.118207.
Liyanage, P.J., Solairaj, S., Arachchilage, G.W., Linnemeyer, H.C., Kim, D.H., Weerasooriya, U., Pope, G.A., 2012. Alkaline surfactant polymer flooding using a novel class of large hydrophobe surfactants. In: SPE Improved Oil Recovery Symposium. https://doi.org/10.2118/154274-MS.
Lu, J., Britton, C., Solairaj, S., Liyanage, P.J., Kim, D.H., Adkins, S., Arachchilage, G.W.P., Weerasooriya, U., Pope, G.A., 2014a. Novel large-hydrophobe alkoxy carboxylate surfactants for enhanced oil recovery. SPE J. 19 (6), 1024–1034. https://doi.org/10.2118/154261-PA.
Lu, J., Weerasooriya, U.P., Pope, G.A., 2014b. Investigation of gravity-stable surfactant floods. Fuel 124. https://doi.org/10.1016/j.fuel.2014.01.082.
Luhning, R.W., Das, S.K., Fisher, L.J., Bakker, J., Grabowski, J., Engleman, J.R., Wong, S., Sullivan, L.A., Boyle, H.A., 2003. Full scale VAPEX process-climate change advantage and economic consequences A. J. Can. Petrol. Technol. 42 (2). https://doi.org/10.2118/03-02-02.
Magzymov, D., Qiao, C.H., Johns, R.T., 2016. Impact of surfactant mixtures on microemulsion phase behavior. In: SPE Annual Technical Conference and Exhibition. https://doi.org/10.2118/181651-MS.
Magzymov, D., Clemens, T., Schumi, B., Johns, R.T., 2021. Experimental analysis of alkali-brine-alcohol phase behavior with high acid number crude oil. SPE Reservoir Eval. Eng. 24 (2), 390–408. https://doi.org/10.2118/201369-PA.
Nadeeka, U., Karasinghe, A., Liyanage, P.J., Jang, S.H., Shook, E., Weerasooriya, U.P., Pope, G.A., 2018. New surfactants and cosolvents increase oil recovery and reduce cost. SPE J. 23 (6), 2202–2217. https://doi.org/10.2118/179702-PA.
Najafi, S.A.S., Kamranfar, P., Madani, M., Shadadeh, M., Jamialahmadi, M., 2017. Experimental and theoretical investigation of CTAB microemulsion viscosity in the chemical enhanced oil recovery process. J. Mol. Liq. 232, 382–389. https://doi.org/10.1016/j.molliq.2017.02.092.
Pei, H.H., Zhang, G.C., Ge, J.J., Tang, M.G., Zheng, Y.F., 2012. Comparative effectiveness of alkaline flooding and alkaline–surfactant flooding for improved heavy-oil recovery. Energy Fuels 26 (5), 2911–2919. https://doi.org/10.1021/ef300206u.
Pei, H.H., Zhang, G.C., Ge, J.J., Zhang, L., Ma, M.C., 2014. Effect of the addition of low molecular weight alcohols on heavy oil recovery during alkaline flooding. Ind. Eng. Chem. Res. 53 (4), 1301–1307. https://doi.org/10.1021/ie4028318.
Quintero, L., 2020. A review on fluids technology for near-wellbore remediation. In: SPE Latin American and Caribbean Petroleum Engineering Conference. https://doi.org/10.2118/199079-MS.
Quintero, L., Jones, T.A., Clark, D.E., Schwertner, D., 2009. Cases history studies of production enhancement in cased hole wells using microemulsion fluids. In: 8th European Formation Damage Conference. https://doi.org/10.2118/121926-MS.
Quintero, L., Felipe, M.J., Miller, K., Ponnapati, R., Loya, M., 2018. Microemulsion increase well productivity by removing organic deposits and inorganic scale in one step. In: SPE International Conference and Exhibition on Formation Damage Control. https://doi.org/10.2118/189514-MS.
Raimondi, P., Gallagher, B.J., Ehrlich, R., Messmer, J.H., Bennett, G.S., 1977. Alkaline waterflooding-design and implementation of a field pilot. J. Petrol. Technol. 29, 1359–1368. https://doi.org/10.2118/5831-PA.
Rousseau, D., Bekri, S., Boujlel, J., Hocine, S., Degre, G., 2018. Designing surfactant-polymer processes for heavy oil reservoirs: case studies. In: SPE Canada Heavy Oil Technical Conference. https://doi.org/10.2118/189745-MS.
Sahni, V., Dean, R.M., Britton, C., Kim, D., Weerasooriya, U., Pope, G.A., 2010. The role of co-solvents and co-surfactants in making chemical floods robust. In: SPE Improved Oil Recovery Symposium. https://doi.org/10.2118/130007-MS.
Sander, R., Connell, L.D., Camilleri, M., et al., 2020. CH_4, CO_2, N_2 diffusion in Bowen Basin (Australia) coal: relationship between sorption kinetics of coal core and crushed coal particles. J. Nat. Gas Sci. Eng. 81, 103468. https://doi.org/10.1016/j.jngse.2020.103468.
Schumi, B., Clemens, T., Wegner, J., Ganzer, L., Kaiser, A., Hincapie, R.E., Leitenmuller, V., 2020. Alkali/cosolvent/polymer flooding of high-TAN oil: using phase experiments, micromodels, and corefloods for injection-agent selection. SPE Reservoir Eval. Eng. 23 (2), 463–478. https://doi.org/10.2118/195504-PA.
Sharma, H., Panthi, K., Mohanty, K.K., 2018. Surfactant-less alkali-cosolvent-polymer floods for an acidic crude oil. Fuel 215, 484–491. https://doi.org/10.1016/j.fuel.2017.11.079.
Sim, S.S., Wassmuth, F.R., Bai, Ji, 2014. Identification of Winsor type III microemulsion for chemical EOR of heavy oil. In: SPE Heavy Oil Conference-Canada. https://doi.org/10.2118/170018-MS.
Su, H., Zhou, F.J., Zheng, A., Wang, L.D., Wang, C., Yu, F.W., Kang, L.X., Li, J.J., 2022. Heavy oil recovery by alkaline-cosolvent-polymer flood: a multiscale research using micromodels and computed tomography imaging. SPE J. 27 (3), 1480–1492. https://doi.org/10.2118/204766-PA.
Tagavifar, M., Xu, K., Jang, S.H., Balhoff, M.T., Pope, G.A., 2017a. Spontaneous and flow-driven interfacial phase change: dynamics of microemulsion formation at the pore scale. Langmuir 33 (45), 13077–13086. https://doi.org/10.1021/acs.langmuir.7b02856.
Tagavifar, M., Herath, S., Weerasooriya, U.P., Sepehrnoori, K., Pope, G.A., 2017b. Measurement of microemulsion viscosity and its implications for chemical enhanced oil recovery. SPE J. 23 (1), 66–83. https://doi.org/10.2118/179672-PA.
Walker, D.L., Britton, C., Kim, D.H., Dufour, S., Weerasooriya, U., Pope, G.A., 2012. The impact of microemulsion viscosity on oil recovery. In: SPE Improved Oil Recovery Symposium. https://doi.org/10.2118/154275-MS.
Wassmuth, F.R., Green, K., Hodgins, L., Turta, A.T., 2007. Polymer flood technology for heavy oil recovery. In: Canadian International Petroleum Conference. https://doi.org/10.2118/2007-182.
Wassmuth, F.R., Arnold, W., Green, K., Cameron, N., 2009. Polymer flood application to improve heavy oil recovery at East Bodo. J. Can. Petrol. Technol. 48 (2), 55–61. https://doi.org/10.2118/09-02-55.
Wei, C.P., Li, W.Z., Wu, G.H., et al., 2020. EOR mechanism of viscosity reducer flooding in heavy oil reservoirs. Editorial Department of Petroleum Geology and Recovery Efficiency 27 (2), 131–136. https://doi.org/10.13673/j.cnki.cn37-1359/te.2020.02.017 (in Chinese).
Wu, Y.G., Dong, M.Z., Shirif, E., 2011. Study of alkaline/polymer flooding for heavy-oil recovery using channeled sandpacks. SPE Reservoir Eval. Eng. 14 (3), 310–319. https://doi.org/10.2118/137460-PA.
Yang, H., Britton, C., Liyanage, P.J., Solairaj, S., Kim, D.H., Nguyen, Q., Weerasooriya, U., Pope, G.A., 2010. Low-cost, high-performance chemicals for enhanced oil recovery. In: SPE Improved Oil Recovery Symposium. https://doi.org/10.2118/129978-MS.
Zhang, J.Y., Ravikiran, R., Freiberg, D., Thomas, C., 2012. ASP formulation design for heavy oil. In: SPE Improved Oil Recovery Symposium. https://doi.org/10.2118/153570-MS.
Zhao, X., Feng, Y., Liao, G., Liu, W., 2020. Visualizing in-situ emulsification in porous media during surfactant flooding: a microfluidic study. J. Colloid Interface Sci. 578, 629–640. https://doi.org/10.1016/j.jcis.2020.06.019.
Zhao, X., Zhan, F., Liao, G., Liu, W., Su, X., Feng, Y., 2022. In situ micro-emulsification during surfactant enhanced oil recovery: a microfluidic study. J. Colloid Interface Sci. 620, 465–477. https://doi.org/10.1016/j.jcis.2022.04.045.
Zhu, T., Kang, W., Yang, H., Li, Z., Zhou, B., He, Y., Wang, J., Aidarova, S., Sarsenbekuly, B., 2022. Advances of microemulsion and its applications for improved oil recovery. Adv. Colloid Interface Sci. 299, 102527. https://doi.org/10.1016/j.cis.2021.102527.